Mie scattering in the time domain. Part II. The role of diffraction

James A. Lock[1,*] and Philip Laven[2]

[1]*Department of Physics, Cleveland State University, Cleveland, Ohio 44115, USA*
[2]*9 Russells Crescent, Horley RH6 7DJ, United Kingdom*
**Corresponding author: j.lock@csuohio.edu*

Received February 15, 2011; accepted March 16, 2011;
posted April 4, 2011 (Doc. ID 142611); published May 18, 2011

The $p = 0$ term of the Mie–Debye scattering amplitude contains the effects of external reflection and diffraction. We computed the reflected intensity in the time domain as a function of the scattering angle and delay time for a short electromagnetic pulse incident on a spherical particle and compared it to the predicted behavior in the forward-focusing region, the specular reflection region, and the glory region. We examined the physical consequences of three different approaches to the exact diffraction amplitude, and determined the signature of diffraction in the time domain. The external reflection surface wave amplitude gradually replaces the diffraction amplitude in the angular transition region between forward-focusing and the region of specular reflection. The details of this replacement were studied in the time domain.

OCIS codes: 260.1960, 290.4020, 320.2250.

1. INTRODUCTION

We know on a qualitative and intuitive basis that when light waves pass closely by the edge of an aperture or obstacle, it is as if the waves bend around the edge and interfere with forward-propagating light that misses the edge by a large distance [1]. This phenomenon is known as diffraction. One may straightforwardly derive the familiar but approximate formulas of Fraunhofer and Fresnel diffraction using the Huygens' construction [2] or the Kirchhoff diffraction integral [3]. But subtle difficulties arise when one attempts to define diffraction in the context of an exactly soluble electromagnetic boundary value problem. For example, the exact solution for the total fields can be obtained when an electromagnetic plane wave is incident on an infinitesimally thin and perfectly conducting half-plane [4]. The exact fields are smoothly varying functions of position. Based on intuitive ideas from geometrical optics, one may decompose these exact wave fields into the incident plane wave in the illuminated region, plus the reflected plane wave in the region of geometrical reflection, plus the remainder. The remainder portion is defined as the diffracted fields, which serve to smooth the transition of the total fields from one geometrical region to another [5]. But, in this decomposition, the geometrical fields possess a discontinuous jump at the edges of the region of their validity [6]. As a result, the diffracted fields possess an equal and opposite discontinuous jump in order to preserve the smoothness of the total fields [7]. As a consequence of this unappealing feature of the exact diffracted fields, various approximations to the exact fields in which the discontinuity has been smoothed over, such as Fraunhofer and Fresnel diffraction, have great practical utility.

The Mie infinite series of partial waves provides an exact solution to the electromagnetic boundary value problem of a plane wave scattered by a spherical particle [8–10]. Each of the Mie partial wave scattering amplitudes may be written as an infinite series, called the Debye series [11], whose terms are identified with the geometrical ray processes of (i) external reflection, (ii) transmission, (iii) transmission following a given number of internal reflections, as applied to the interaction of partial waves with the sphere surface, and (iv) a remainder term. The remainder term is independent of the particle's composition and depends only on its size. As was the case for the half-plane geometry, the remainder term is again the definition of diffraction for this scattering geometry, and is sometimes called the classical diffraction amplitude [12–15]. This diffraction amplitude also has certain unappealing features. Specifically, although it is a smoothly varying function of the scattering angle, its dependence on the sphere radius contains discontinuous jumps. The purposes of this paper are to (i) study the physical implications of the exact diffraction amplitude, (ii) see how various approximations to diffraction smooth these discontinuities, and (iii) show how the features of diffraction manifest themselves in the time domain when a short electromagnetic pulse is scattered by a spherical particle.

The body of this paper is organized as follows. In Section 2, we briefly describe the decomposition of the $p = 0$ Mie–Debye scattering amplitude into three physical processes: (i) diffraction, (ii) external reflection, and (iii) grazing-plus-tunneling reflection. In Section 3, we outline the calculation of reflection and grazing-plus-tunneling reflection in the forward-focusing region $\theta < 1/ka$, the specular reflection region $\theta > (2/ka)^{1/3}$, and the glory region $\theta \approx \pi$, and determine the signature of reflection in the time domain. In Section 4, we approach the exact diffraction amplitude of Section 2 in three different ways and discuss the physical interpretation resulting from each approach. We also compute and interpret the signature of the exact diffraction amplitude in the time domain. We find that the exact definition of diffraction gives rise to what may be interpreted as an orbiting behavior that would seem to violate the causality condition for scattering [16]. In Section 5, we outline the procedure by which the external reflection

electromagnetic surface wave amplitude gradually replaces the diffraction amplitude in the angular region between forward focusing and specular reflection so as to eliminate the apparent causality violation, and we illustrate the details of the replacement in the time domain. Lastly, in Section 6, we summarize our major results.

2. DECOMPOSITION OF THE $p = 0$ TERM OF THE DEBYE SERIES

When an electromagnetic plane wave of wavelength λ, wave number $k = 2\pi/\lambda$, electric field strength E_0, polarized in the x direction, and propagating in the positive z direction is incident on a spherical particle of radius a and refractive index N, the far-zone scattered electric field in Mie theory is [8–10]

$$\mathbf{E}^{\text{scatt}}(\theta,\varphi) = \mathrm{i}S_2(\theta)\cos(\varphi)\mathbf{u}_{\boldsymbol{\theta}} - \mathrm{i}S_1(\theta)\sin(\varphi)\mathbf{u}_{\varphi}, \tag{1}$$

where the scattering amplitudes are

$$S_1(\theta) = \sum_{n=1}^{\infty}\{(2n+1)/[n(n+1)]\}[a_n\pi_n(\theta) + b_n\tau_n(\theta)], \tag{2a}$$

$$S_2(\theta) = \sum_{n=1}^{\infty}\{(2n+1)/[n(n+1)]\}[a_n\tau_n(\theta) + b_n\pi_n(\theta)]. \tag{2b}$$

The $E_0[\exp(\mathrm{i}kr - \mathrm{i}\omega t)]/(kr)$ dependence of the outgoing spherical wave has been suppressed in Eq. (1). The $p = 0$ portion of the Debye series decomposition of the Mie theory partial wave scattering amplitudes is [14]

$$a_n = (1/2)(1 - R_n^{\text{TM}}), \tag{3a}$$

$$b_n = (1/2)(1 - R_n^{\text{TE}}), \tag{3b}$$

where the partial wave external reflection amplitudes R_n^{TE} and R_n^{TM} are quotients of sums of products of Riccati–Bessel and Riccati–Neumann functions evaluated at ka and Nka. Equations (3a) and (3b) describe diffraction plus external reflection in the short wavelength limit $\lambda \ll a$. For the remainder of this paper, we define diffraction to be [12,14]

$$S_1^{\text{diff}}(\theta) = S_2^{\text{diff}}(\theta) = (1/2)\sum_{n=1}^{kA}\{(2n+1)/[n(n+1)]\}[\pi_n(\theta) + \tau_n(\theta)]. \tag{4}$$

Since the partial wave numbers n are constrained to be integers, the upper limit of the partial wave sum is kA, the greatest integer contained in the particle size parameter ka. This causes discontinuous jumps in the dependence of diffraction on particle size. The diffraction amplitudes change only when ka passes an integer value and the contribution of one additional partial wave is added to the sum.

The details of external reflection are intimately related to the angular interval under consideration and the impact parameter with which an effective geometrical ray strikes the sphere [17–19]. Geometrical rays striking the sphere surface with nongrazing incidence are reflected in the nonforward direction, $\theta > (2/ka)^{1/3}$. The scattering amplitudes for this physical process of specular reflection are

$$S_1^{\text{ref}}(\theta) = (-1/2)\sum_{n=1}^{[ka-\varepsilon_{\max}(ka)^{1/3}]-1}\{(2n+1)/[n(n+1)]\}[R_n^{\text{TM}}\pi_n(\theta) + R_n^{\text{TE}}\tau_n(\theta)], \tag{5a}$$

$$S_2^{\text{ref}}(\theta) = (-1/2)\sum_{n=1}^{[ka-\varepsilon_{\max}(ka)^{1/3}]-1}\{(2n+1)/[n(n+1)]\}[R_n^{\text{TM}}\tau_n(\theta) + R_n^{\text{TE}}\pi_n(\theta)], \tag{5b}$$

where $[x]$ denotes the greatest integer contained in x. Partial waves with $n + 1/2 = (ka) + \varepsilon(ka)^{1/3}$ and $-\varepsilon_{\max} \le \varepsilon \le \varepsilon_{\max}$ correspond to rays that either strike the sphere with grazing incidence, or classically just miss striking the sphere's surface, tunnel through the centrifugal barrier surrounding it, and nonetheless reflect from the sphere surface [13,14]. These partial waves are said to be in the edge region. The scattering amplitudes for the physical process of grazing-plus-tunneling reflection of the partial waves in the edge region are

$$\begin{aligned} S_1^{\text{graz+tunn}}(\theta) = (-1/2)&\sum_{n=[ka-\varepsilon_{\max}(ka)^{1/3}]}^{kA}\{(2n+1)/[n(n+1)]\} \\ &\times [R_n^{\text{TM}}\pi_n(\theta) + R_n^{\text{TE}}\tau_n(\theta)] + (1/2) \\ &\times \sum_{n=kA+1}^{[ka+\varepsilon_{\max}(ka)^{1/3}]}\{(2n+1)/[n(n+1)]\}[(1-R_n^{\text{TM}})\pi_n(\theta) \\ &+ (1-R_n^{\text{TE}})\tau_n(\theta)], \end{aligned} \tag{6a}$$

$$\begin{aligned} S_2^{\text{graz+tunn}}(\theta) = (-1/2)&\sum_{n=[ka-\varepsilon_{\max}(ka)^{1/3}]}^{kA}\{(2n+1)/[n(n+1)]\} \\ &\times [R_n^{\text{TM}}\tau_n(\theta) + R_n^{\text{TE}}\pi_n(\theta)] + (1/2) \\ &\times \sum_{n=kA+1}^{[ka+\varepsilon_{\max}(ka)^{1/3}]}\{(2n+1)/[n(n+1)]\}[(1-R_n^{\text{TM}})\tau_n(\theta) \\ &+ (1-R_n^{\text{TE}})\pi_n(\theta)]. \end{aligned} \tag{6b}$$

In Eqs. (6a) and (6b), the first sum is the contribution of grazing incidence and the second sum is the contribution of effective rays that just miss striking the sphere and tunnel through the centrifugal barrier.

That the combination of grazing reflection and tunneling reflection should be thought of as a single physical process is suggested by the limiting behaviors of the various contributions. First, if the Riccati–Bessel and Riccati–Neumann functions in R_n^{TE} and R_n^{TM} are replaced by their asymptotic forms for $\varepsilon \gg 0$ at the upper end of the edge region [20], one obtains

$$R_n^{\text{TE}} = R_n^{\text{TM}} \to 1 - \mathrm{i}\exp(-2^{5/2}\varepsilon^{3/2}/3) + O[1/(ka)^{1/3}] \tag{7}$$

independent of refractive index. Equation (7) is the wave optics equivalent of the geometrical ray Fresnel external reflection coefficient approaching -1 independent of refractive index as the angle of ray incidence approaches 90°. This behavior does not produce convergence of the partial wave sum for reflection alone as $n \to \infty$. In order to obtain convergence for $\varepsilon \gg 0$, one needs to use the full $p = 0$ amplitude [17–19]

$$1 - R_n^{\text{TE}} = 1 - R_n^{\text{TM}} \to \mathrm{i}\exp(-2^{5/2}\varepsilon^{3/2}/3) + O[1/(ka)^{1/3}]. \tag{8}$$

Second, if the Riccati–Bessel functions in R_n^{TE} and R_n^{TM} are replaced by their asymptotic forms for $\varepsilon \ll 0$ at the lower end of the edge region [21], one obtains

$$-R_n^{\mathrm{TE}} = -R_n^{\mathrm{TM}} \to \mathrm{i}\exp(-\mathrm{i}2^{5/2}|\varepsilon|^{3/2}/3) + O[1/(ka)^{1/3}]. \quad (9)$$

Equations (8) and (9) have the same functional form in the $\varepsilon \gg 0$ and $\varepsilon \ll 0$ limits, again suggesting that, for scattering in the short wavelength limit, it is natural to consider the combination of grazing reflection and tunneling reflection for partial waves in the edge region as a single physical process.

3. REFLECTED PORTION OF THE $p = 0$ DEBYE SERIES TERM

We first consider specular reflection in the angular interval $\theta > (2/ka)^{1/3}$. The Riccati–Bessel and Riccati–Neumann functions in R_n^{TE} and R_n^{TM} in Eqs. (5a) and (5b) are replaced by their large-order large-argument approximation [22]. The angular functions $\pi_n(\theta)$ and $\tau_n(\theta)$ in this angular interval [23] are expanded in powers of $n + 1/2$ and the leading term is retained. The resulting partial wave sum is approximated by an integral over an effective impact parameter [24], and the integral is then evaluated using the method of stationary phase. As long as $\theta > (2/ka)^{1/3}$, the stationary phase point falls well within the range of partial waves considered. The result is the ray optics scattering amplitude

$$S_1^{\mathrm{ref}}(\theta) = \mathrm{i}(ka/2)r^{\mathrm{TE}}(\theta)\exp[-2\mathrm{i}ka\sin(\theta/2)], \quad (10a)$$

$$S_2^{\mathrm{ref}}(\theta) = \mathrm{i}(ka/2)r^{\mathrm{TM}}(\theta)\exp[-2\mathrm{i}ka\sin(\theta/2)], \quad (10b)$$

along with various wave optics corrections. The external reflection Fresnel coefficients in Eqs. (10a) and (10b) are

$$r^{\mathrm{TE}}(\theta) = \{[N^2 - \cos^2(\theta/2)]^{1/2} - \sin(\theta/2)\}/\{[N^2 - \cos^2(\theta/2)]^{1/2} + \sin(\theta/2)\}, \quad (11a)$$

$$r^{\mathrm{TM}}(\theta) = \{[N^2 - \cos^2(\theta/2)]^{1/2} - N^2\sin(\theta/2)\}/\{[N^2 - \cos^2(\theta/2)]^{1/2} + N^2\sin(\theta/2)\}. \quad (11b)$$

Consider a plane wave pulse $\mathbf{E}^{\mathrm{pulse}}(z,t)$ with the Fourier spectrum $A(k)$ incident on the sphere. The reflected electric field in the time domain is obtained [25–28] by inverse Fourier transforming the product of the scattered field of Eqs. (10a) and (10b) and the incident pulse spectrum, giving

$$\mathbf{E}^{\mathrm{ref}}(t,\theta,\varphi) = [-r^{\mathrm{TM}}(\theta)\cos(\varphi)\mathbf{u}_{\boldsymbol{\theta}} + r^{\mathrm{TE}}(\theta)\sin(\varphi)\mathbf{u}_{\varphi}] \times \int_{-\infty}^{\infty}(\mathrm{d}k/2\pi)A(k)(ka/2)\exp[-2\mathrm{i}ka\sin(\theta/2) - \mathrm{i}ckt]. \quad (12)$$

For a temporal Gaussian pulse with the spectrum function

$$A(k) = \sigma(\pi)^{1/2}\exp[-\sigma^2(k-k_0)^2/4], \quad (13)$$

the magnitude-squared of the time domain electric field can be evaluated analytically and gives the intensity

$$I^{\mathrm{ref}}(t,\theta,\varphi) = [(k_0a)^2/4]\{[r^{\mathrm{TE}}(\theta)]^2\cos^2(\varphi) + [r^{\mathrm{TM}}(\theta)]^2\sin^2(\varphi)\} \times \exp\{-2[ct + 2a\sin(\theta/2)]^2/\sigma^2\}, \quad (14)$$

where the $E_0^2/(k_0r)^2$ dependence is suppressed in Eq. (14). This prediction is compared in Fig. 1 with the numerically computed $p = 0$ time domain intensity using the 10 fs wide raised cosine pulse of [29] with $\lambda_0 = 0.65\,\mu$m incident on a spherical particle of radius $a = 10\,\mu$m and refractive index $N + \mathrm{i}K = 1.3326 + \mathrm{i}(1.67 \times 10^{-8})$. As was the case in [29], in this paper, all the analytical results are obtained using the Gaussian pulse, whereas all the numerical results are obtained using the truncated raised cosine pulse. The behavior of the relative maximum of the time domain intensity is independent of pulse shape. In addition, it should be noted that the delay times in Fig. 1 are given relative to that of the externally reflected central ray. For future reference, the temporal maximum of the reflected pulse without the offset of Fig. 1 added on is given in the time domain by

$$t = -(2a/c)\sin(\theta/2) \approx -a\theta/c \quad (15)$$

when θ is small.

Grazing-plus-tunneling reflection of the edge rays contributes to scattering at all angles. In the forward-focusing region

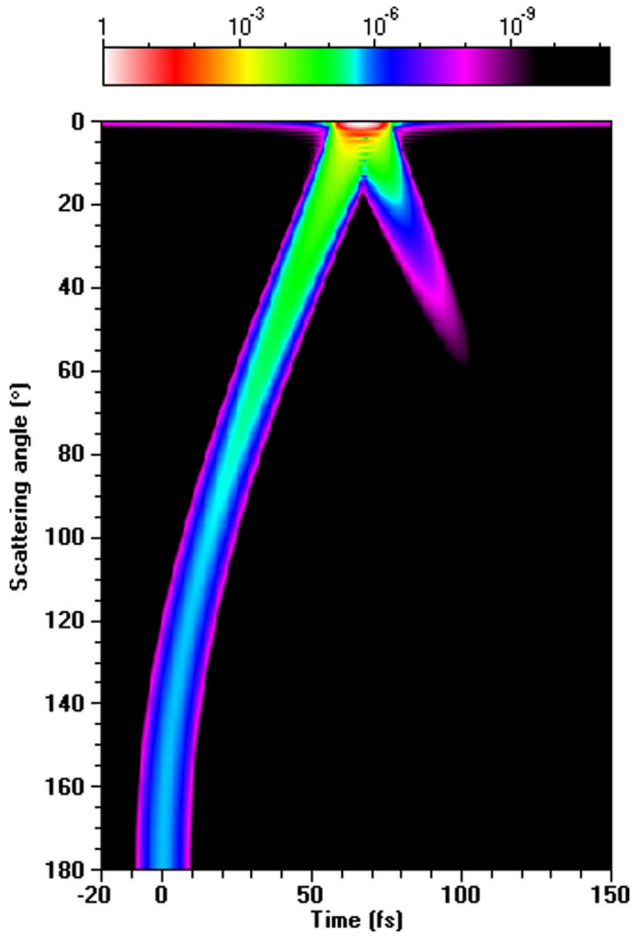

Fig. 1. (Color online) Intensity of the $p = 0$ Mie–Debye term as a function of the scattering angle and delay time for the unpolarized raised cosine pulse of [29] with $\lambda_0 = 0.65\,\mu$m. and $\tau = 5$ fs incident on a spherical particle of radius $a = 10\,\mu$m and refractive index $N + \mathrm{i}K = 1.3326 + \mathrm{i}(1.67 \times 10^{-8})$.

$\theta < 1/ka$, keeping the first two terms in the expansion of R_n^{TE} and R_n^{TM} in powers of ka in Eqs. (6a) and (6b), using the appropriate approximation to the angular functions [12], and approximating the sum over partial waves by an integral over ε, we obtain the transitional approximation to the externally reflected field

$$\begin{aligned}\mathbf{E}^{\mathrm{graz+tunn}}(\theta,\varphi) = \{&(ka)^{4/3}\exp(5\pi\mathrm{i}/6)\\ &+ (ka)(N^2+1)/[2(N^2-1)^{1/2}]\}J_0(ka\theta)\mathbf{u_x}\\ &- [(ka)(N^2-1)^{1/2}J_2(ka\theta)/2]\\ &\times[\cos(2\varphi)\mathbf{u_x}+\sin(2\varphi)\mathbf{u_y}].\end{aligned} \tag{16}$$

The $(ka)^{4/3}$ dependence of the leading term is characteristic of constructive interference of an effective ring source of width $(ka)^{1/3}$ located on the circular locus of grazing incidence points [30] and represents a focusing amplification beyond the $(ka)^1$ geometrical optics background of Eqs. (10a) and (10b).

For grazing-plus-tunneling reflection of the edge rays in the specular reflection region $\theta > (2/ka)^{1/3}$, the first two terms in the expansion of R_n^{TE} and R_n^{TM} in powers of ka in Eqs. (6a) and (6b) are used along with the $\exp[\mathrm{i}(n+1/2)\theta - \mathrm{i}\pi/4]$ portion of the angular functions of [23], and the sum over partial waves is again approximated by an integral over ε. The integration region is then extended to the entire ε axis in order to obtain a contour integral in the complex plane, which is then evaluated using the method of residues. The resulting transitional approximation to the surface wave portion of the external reflection field is

$$\begin{aligned}\mathbf{E}^{\mathrm{graz+tunn}}(\theta,\varphi) = &(ka)^{5/6}T(\theta)B(k,\theta)\exp[\mathrm{i}ka\Phi(k,\theta)]\\ &\times\{[1-N^2\theta/(N^2-1)^{1/2}]\cos(\varphi)\mathbf{u_\theta}\\ &-[1-\theta/(N^2-1)^{1/2}]\sin(\varphi)\mathbf{u}_\varphi\},\end{aligned} \tag{17}$$

where

$$T(\theta) = \exp(7\mathrm{i}\pi/12)/\{2^{5/6}[\pi\sin(\theta)]^{1/2}[\mathrm{Ai}'(-X)]^2\}, \tag{18}$$

$$\begin{aligned}B(k,\theta) = \exp\{&-\theta[3^{1/2}X(ka)^{1/3}/2^{4/3}\\ &-(1/2)(N^2+1)/(N^2-1)^{1/2}]\},\end{aligned} \tag{19}$$

$$\Phi(k,\theta) = \theta\{1+X/[2^{4/3}(ka)^{2/3}]\}. \tag{20}$$

In Eqs. (18)–(20), $X = 2.3381$ is the magnitude of the argument of the first zero of the Airy function [31], which occurs in the residue of the dominant pole of the integrand. In Eq. (19), the weak polarization dependence of the damping rate [19] has been replaced by the average damping rate. The first two terms of the reflected ray portion of the scattered field are obtained from the $\exp[-\mathrm{i}(n+1/2)\theta + \mathrm{i}\pi/4]$ portion of the angular functions and a stationary phase evaluation of the resulting integral. The result coincides with the first two terms of Eqs. (10a) and (10b) when expanded in powers of θ. Multiplying Eqs. (17)–(20) by the spectrum function of the incident pulse and inverse Fourier transforming the result, one obtains the surface wave field in the time domain. Ignoring the dispersion of the surface wave speed in Eq. (20), the surface wave intensity in the time domain is then

$$\begin{aligned}I^{\mathrm{graz+tunn}}(t,\theta,\varphi) = (k_0a)^{5/3}&[T(\theta)B(k_0,\theta)]^2\exp\{-2[ct\\ &-a\Phi(k_0,\theta)]^2/\sigma^2\}.\end{aligned} \tag{21}$$

The temporal maximum of the surface wave pulse occurs at

$$t = (a\theta/c)\{1+X/[2^{4/3}(k_0a)^{2/3}]\}. \tag{22}$$

For grazing-plus-tunneling reflection of the edge rays in the glory region $\theta \approx \pi - \delta$, where δ is a small angle, the method described above along with the approximation of [32] to the angular functions and applied to Eqs. (6a) and (6b) for both the shorter path and longer path surface waves gives the surface wave glory:

$$\begin{aligned}\mathbf{E}^{\mathrm{graz+tunn}}(\theta,\varphi) = &(ka)^{4/3}\{\exp(-4\mathrm{i}\pi/3)B(k,\pi)\\ &\times\exp[\mathrm{i}ka\Phi(k,\pi)]/2^{1/3}[\mathrm{Ai}'(-X)]^2\}\\ &\times\{[-\pi(N^2-1)^{1/2}/2]J_0(ka\delta)\mathbf{u_x}\\ &+[1+\pi(N^2+1)/2(N^2-1)^{1/2}]J_2(ka\delta)\\ &\times[\cos(2\varphi)\mathbf{u_x}+\sin(2\varphi)\mathbf{u_y}]\}.\end{aligned} \tag{23}$$

The slow angular dependence of the surface wave damping has been evaluated at $\theta = \pi$ in Eq. (23), while the rapid angular dependence of the Bessel functions has been retained. The surface wave glory is amplified by a factor of $(ka)^{1/2}$ above that of Eq. (17) for angles below the glory region.

4. DIFFRACTED PORTION OF THE $p = 0$ DEBYE SERIES TERM

Diffraction was defined in Eq. (4) as the portion of the electromagnetic wave scattering amplitude that is independent of the particle's composition. Since the angular functions $\pi_n(\theta)$ and $\tau_n(\theta)$ are derivatives of Legendre polynomials $P_n[\cos(\theta)]$, substitution of the resulting expression for $\pi_n(\theta)+\tau_n(\theta)$ into the Legendre polynomial differential equation [33] gives

$$\begin{aligned}S_{\mathrm{em}}^{\mathrm{diff}}(\theta) = &\sum_{n=1}^{kA}(n+1/2)P_n[\cos(\theta)]\\ &+[1-\cos(\theta)]\sum_{n=1}^{kA}\{(n+1/2)/[n(n+1)]\}\\ &\times \mathrm{d}P_n[\cos(\theta)]/\mathrm{d}\cos(\theta).\end{aligned} \tag{24}$$

The first sum in Eq. (24) coincides with the definition of diffraction for scattering of scalar waves by a sphere [17] except that $n = 0$ is also included for scalar waves, and the second sum describes additional differences between diffraction of electromagnetic waves and diffraction of scalar waves.

Three different approaches to Eq. (4) are now pursued in order to elucidate a number of features of diffraction. First, one may substitute $\pi_n(\theta)$ and $\tau_n(\theta)$ obtained from the uniform asymptotic approximation of the Legendre polynomials [34] for arbitrary n,

$$\begin{aligned}P_n[\cos(\theta)] = &[\theta/\sin(\theta)]^{1/2}\{J_0[(n+1/2)\theta]\\ &+J_1[(n+1/2)\theta][\cot(\theta)-(1/\theta)]/[8(n+1/2)]\\ &+O[1/(n+1/2)^2]\},\end{aligned} \tag{25}$$

into Eq. (4). The uniform approximation diverges as θ approaches 180°, but it is both accurate and useful away from backscattering [35]. When the sum over partial waves is approximated by an integral over an effective impact parameter, the diffraction amplitude for electromagnetic waves becomes

$$S_{\mathrm{em}}^{\mathrm{diff}}(\theta) \approx [\theta/\sin(\theta)]^{1/2}\{(kA)^2 J_1(kA\theta)/(kA\theta) + [1/\sin(\theta) - (1/8\theta) - 7\cot(\theta)/8][1 - J_0(kA\theta)] + O(1/kA)\}, \tag{26}$$

while the first term of Eq. (24) for scattering of scalar waves gives [13]

$$S_{\mathrm{scalar}}^{\mathrm{diff}}(\theta) \approx [\theta/\sin(\theta)]^{1/2}\{(kA)^2 J_1(kA\theta)/(kA\theta) + [-(1/8\theta) + \cot(\theta)/8][1 - J_0(kA\theta)] + O(1/kA)\}. \tag{27}$$

Although the second term in Eqs. (26) and (27) differs from electromagnetic diffraction to scalar wave diffraction, the first term dominates for large kA, and reduces for small θ to the familiar Fraunhofer diffraction amplitude

$$S^{\mathrm{diff}}(\theta) \approx (ka)^2 J_1(ka\theta)/(ka\theta) \tag{28}$$

when A is replaced by the actual particle radius a, thus smoothing the dependence on particle size.

As a second approach to Eq. (4), we instead use the Taylor series expansion of the Legendre polynomials about $\theta = 0°$ [36],

$$P_n[\cos(\theta)] = 1 - n(n+1)\theta^2/4 + [n(n+1)/48 + (n-1)n(n+1)(n+2)/64]\theta^4 + O(\theta^6). \tag{29}$$

For small scattering angles, Eq. (29) is found to be less complicated than attempting to Taylor series expand the uniform approximation of Eq. (25). Substituting $\pi_n(\theta)$ and $\tau_n(\theta)$ obtained from Eq. (29) into Eq. (4) and performing the resulting sums over partial waves exactly gives

$$S_{\mathrm{em}}^{\mathrm{diff}}(\theta) = [kA(kA+2)/2]\{1 - (\theta^2/8)[(kA)^2 + 2kA - 1] + O(\theta^4)\}. \tag{30}$$

An approximation to Eq. (30) in terms of the Bessel function J_1 and the actual particle radius a is

$$S_{\mathrm{em}}^{\mathrm{diff}}(\theta) \approx (ka+1)^2 J_1[(ka+1)\theta]/[(ka+1)\theta]. \tag{31}$$

For diffraction of scalar waves, substituting $\pi_n(\theta)$ and $\tau_n(\theta)$ obtained from Eq. (29) into the first term of Eq. (24) and performing the sum over partial waves starting with $n = 0$ exactly gives

$$S_{\mathrm{scalar}}^{\mathrm{diff}}(\theta) = [(kA+1)^2/2][1 - kA(kA+2)\theta^2/8 + O(\theta^4)], \tag{32}$$

again leading to the approximation of Eq. (31).

In the short wavelength limit $ka + 1 \approx ka$, we choose to retain the factors of $ka + 1$ in order to motivate the following physical interpretation of diffraction. For $\theta > 2.5/ka$, the asymptotic form [37] of the Bessel function $J_1[(ka+1)\theta]$ is valid and may be substituted into Eq. (31), with the factor $[\theta/\sin(\theta)]^{1/2}$ appended, giving

$$S^{\mathrm{diff}}(\theta) \approx \{(ka+1)/[2\pi\sin(\theta)]\}^{1/2}(1/\theta) \times \{\exp[\mathrm{i}ka\theta(1+1/ka) - 3\mathrm{i}/4] + \exp[-\mathrm{i}ka\theta(1+1/ka) + 3\mathrm{i}/4]\}. \tag{33}$$

The diffracted electric field in this angular region is then proportional to

$$\mathbf{E}^{\mathrm{diff}}(\theta,\varphi) \sim [E_0(ka+1)^{1/2}/kr]\{\exp[\mathrm{i}kr + \mathrm{i}ka\theta(1+1/ka) - \mathrm{i}\omega t] - \mathrm{i}\exp[\mathrm{i}kr - \mathrm{i}ka\theta(1+1/ka) - \mathrm{i}\omega t]\}[\cos(\varphi)\mathbf{u}_{\theta} - \sin(\varphi)\mathbf{u}_{\varphi}]. \tag{34}$$

In the context of the geometrical theory of diffraction [38,39], the two complex exponentials in Eqs. (33) and (34) can be interpreted as the two diffracted rays pictorially illustrated in Fig. 2. The first ray, corresponding to the first complex exponential in Eq. (34), is incident on the entrance plane A′A at the top of the sphere. It then advances its phase by $ka\theta(1+1/ka)$ between the entrance plane and the exit plane B′B, before heading off toward the far zone with the scattering angle θ. In Fig. 2, we pictorially model this phase advance as the diffracted ray traveling for an angular distance θ between the entrance plane and exit plane above the sphere surface at the radius

$$r = a(1+1/ka). \tag{35}$$

The second diffracted ray, corresponding to the second complex exponential in Eq. (34), is assumed to be incident on the entrance plane at the bottom of the sphere with the same phase as that of the first ray. It then retards its phase by $ka\theta(1+1/ka)$ before arriving at the exit plane and then

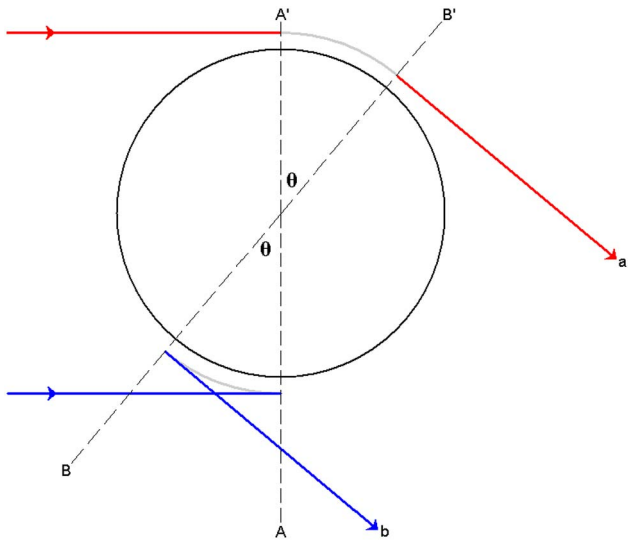

Fig. 2. (Color online) Diffracted rays a and b are assumed to arrive at the entrance plane A′A with the same phase. Then ray a advances its phase by $ka\theta(1+1/ka)$ between the entrance plane and the exit plane B′B for scattering at the angle θ. The diffracted ray b retards its phase by $ka\theta(1+1/ka)$ between the entrance and exit planes.

heading off toward the far zone with the scattering angle θ. In Fig. 2, we pictorially model the phase retardation as the ray traveling in the backward direction between the entrance and exit planes for an angular distance θ above the sphere surface at the radius $r = a(1 + 1/ka)$. We are not implying that the second ray literally turns around, travels backwards for an angle θ, and then turns around again. Rather, we are only reminding the reader that it retards its phase between the entrance plane and exit plane rather than advancing its phase. An analogous interpretation can be made in the geometrical theory of diffraction for the two diffracted rays incident at the top and bottom edges of a slit aperture. In [29], we found that surface waves could also be interpreted as traveling above the sphere surface at the radius $r = a[1 + 0.810/(ka)^{2/3}]$ while tangentially shedding their radiation toward the far zone.

The time domain intensity associated with Eq. (33) for an incident Gaussian pulse is

$$\begin{aligned} I^{\text{diff}}(t,\theta) = \{k_0 a/[2\pi\theta^2 \sin(\theta)]\}\{&\exp[-2(ct - a\theta)^2/\sigma^2] \\ &+ \exp[-2(ct + a\theta)^2/\sigma^2] \\ &- 2\sin(2k_0 a\theta)\exp[-(ct - a\theta)^2/\sigma^2] \\ &\times \exp[-(ct + a\theta)^2/\sigma^2]\}. \end{aligned} \tag{36}$$

The temporal maxima of the diffracted pulses of Eq. (36) are the diagonal straight lines

$$t = \pm a\theta/c, \tag{37}$$

giving the inverted "V"-shaped time domain signature of the two diffracted rays in Fig. 3. The shorter-time arm, however, has the same time domain signature as the near-forward specular reflection in Eq. (15), and the longer-time arm has virtually the same time domain signature as the external reflection surface wave of Eq. (22). This produces the evolution of the shorter-time diffraction arm into the specular reflection curve in Fig. 1 and leads to the shortening of the longer-time diffraction arm via its replacement by external reflection surface waves. The details of this shortening are discussed in more detail in Section 5.

The region of near-forward scattering in the time domain for $p = 0$, $\lambda_0 = 0.65\,\mu$m, and $a = 10\,\mu$m is shown in detail in Fig. 4. The central focusing maximum is evident for $\theta \le 2°$. In the forward-focusing region, corresponding to $\theta < 0.59°$, the diffracted intensity is proportional to $(k_0 a)^4$ with the angular dependence $[J_1(k_0 a\theta)/(k_0 a\theta)]^2$ consistent with Eq. (28). Additional focusing is produced by the dominant term of the grazing-plus-tunneling reflection intensity, which is proportional to $(k_0 a)^{8/3}$ with the angular dependence $[J_0(k_0 a\theta)]^2$ of Eq. (16). For scattering angles in the forward-focusing region, the diffracted intensity of Eq. (36) cannot be expected to be accurate since the approximation of the Bessel function $J_1[k_0 a\theta]$ by its asymptotic form is not warranted. But, for $\theta > 1.5°$, the diffracted intensity is given by Eq. (36). There are intensity minima on the centerline of the inverted V in Fig. 4 at $\theta \approx 2.2°$, 4.0°, 5.6°, and 7.2°. If diffraction alone were present in the form of Eqs. (28) and (33), the minima of the diffraction intensity cross term on the axis of the inverted V should occur at $\theta = 2.27°$, 4.15°, 6.03°, and 7.90°. The first two minima are fit well by diffraction dominance. But grazing-plus-tunneling reflection plays an increasingly important role as

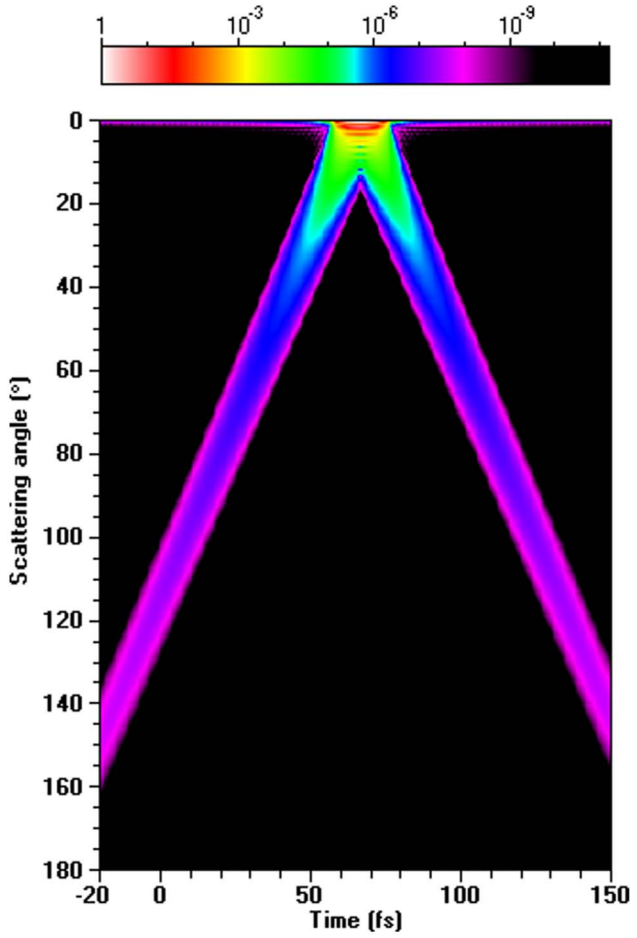

Fig. 3. (Color online) Diffracted intensity corresponding to Eq. (33) as a function of the scattering angle and delay time for the unpolarized raised cosine pulse and spherical particle of Fig. 1.

the scattering angle increases. If the J_0 portion of Eq. (16) for external reflection forward focusing were added to Eq. (33), the predicted minima shift to $\theta = 2.27°$, 4.08°, 5.90°, and 7.70°, in slightly better agreement with the figure. In the specular reflection region, corresponding to $\theta > 15.73°$, the ray intensity is given by Eq. (14) and the external reflection surface wave intensity is given by Eq. (21).

For large scattering angles, Eqs. (19) and (21) indicate that the surface wave intensity dies off exponentially as a function of the scattering angle, while Eq. (36) suggests that the diffracted intensity dies off much more slowly, as $1/\theta^2$. Thus, one might expect, on the basis of Fig. 3, that diffraction extends to larger scattering angles than does the radiation shed by external reflection surface waves. This is not observed in Fig. 1 where the longer-time diffraction arm of the inverted V dies out by $\theta \approx 50°$ and the shorter-time arm diffraction extending to negative times is conspicuously absent. The incorrectness of this expectation is addressed more fully in Section 5.

Although the diffracted field of Eqs. (4) and (24) is largest in the near-forward direction, it extends to all scattering angles, including the backscattering glory region. Such was the case as well for diffraction of a plane wave by the infinitesimally thin and perfectly conducting half-plane [6] in Section 1. For the calculation of diffraction in the glory region, one cannot directly use Eq. (25) due to the divergence of the uniform

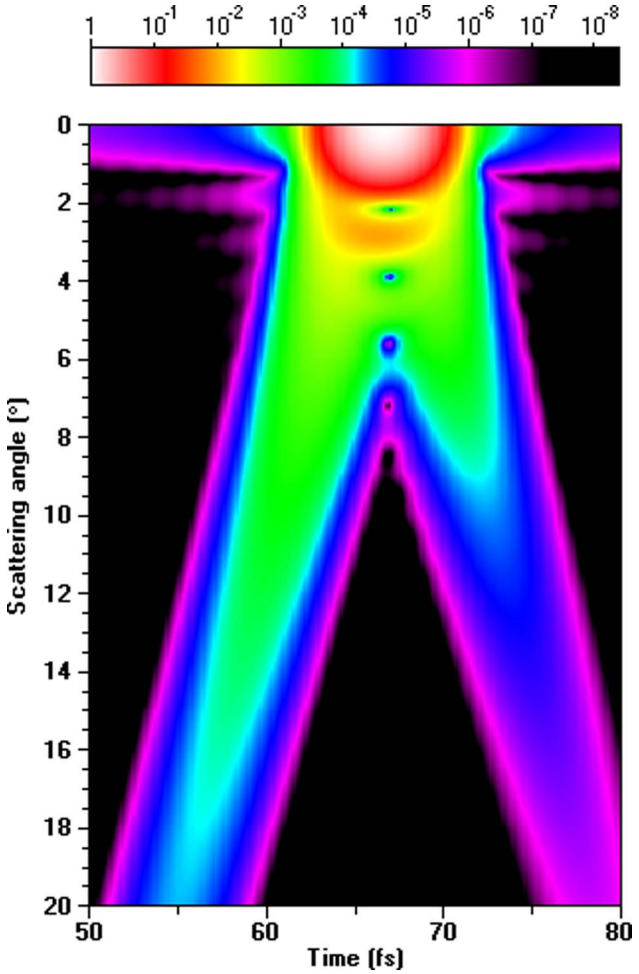

Fig. 4. (Color online) Intensity of the $p = 0$ Mie–Debye term as a function of scattering angle and delay time in the near-forward direction for the unpolarized raised cosine pulse and spherical particle of Fig. 1. The fundamental sampling interval is 0.135 fs.

asymptotic approximation to the Legendre polynomial P_n. Rather, one must first use the identity

$$P_n[\cos(\pi - \delta)] = (-1)^n P_n[\cos(\delta)], \tag{38}$$

and then substitute $\pi_n(\theta)$ and $\tau_n(\theta)$ obtained from either Eq. (25) or Eq. (29) into Eq. (4). Using Eq. (29) and then evaluating the alternating series of partial waves exactly, the scattering amplitude for the diffraction glory for electromagnetic waves is

$$S_{\mathrm{em}}^{\mathrm{diff}}(\theta) = -\exp(\mathrm{i}\pi kA)[kA(kA+1)(kA+2)\delta^2/16 + O(\delta^4)]. \tag{39}$$

This can be approximated in terms of Bessel functions and the actual particle radius as

$$S_{\mathrm{em}}^{\mathrm{diff}}(\theta) \approx -\exp(\mathrm{i}\pi ka)[(ka+1)/2]J_2[(ka+1)\delta]. \tag{40}$$

For scattering of scalar waves, substituting Eqs. (29) and (38) into the first term of Eq. (24) gives

$$S_{\mathrm{scalar}}^{\mathrm{diff}}(\theta) = \exp(\mathrm{i}\pi kA)[(kA+1)/2][1 - \delta^2 kA(kA+2)/4 + O(\delta^4)], \tag{41}$$

$$\approx \exp(\mathrm{i}\pi ka)[(ka+1)/2]J_0[(ka+1)\delta]. \tag{42}$$

The center of the scalar wave diffraction glory should be an intensity maximum, whereas it should be an intensity minimum for the electromagnetic diffraction glory. In addition, the field in the glory region scales as $(ka)^1$ rather than as $(ka)^2$ in the forward direction and is again amplified by a factor of $(ka)^{1/2}$ with respect to diffraction in the specular reflection region of Eq. (33). This weaker focusing is due to the alternating signs of the partial wave contributions in Eq. (38), whereas all the partial wave contributions to the forward-focusing peak have the same sign. The $J_2(k_0 a\delta)$ dependence in the glory region is evident in Fig. 5, where the intensity maxima occur at $\delta \approx 2.5°$, 5.5°, and 8.0°, and the corresponding relative maxima and minima of $J_2(k_0 a\delta)$ occur at $\delta \approx 2.26°$, 4.97°, and 7.39°.

The third approach to the diffraction amplitude makes use of the Poisson sum formula, which, in its usual form [40], equates an infinite series of sampled values of a function to an infinite series of sampled values of its Fourier transform.

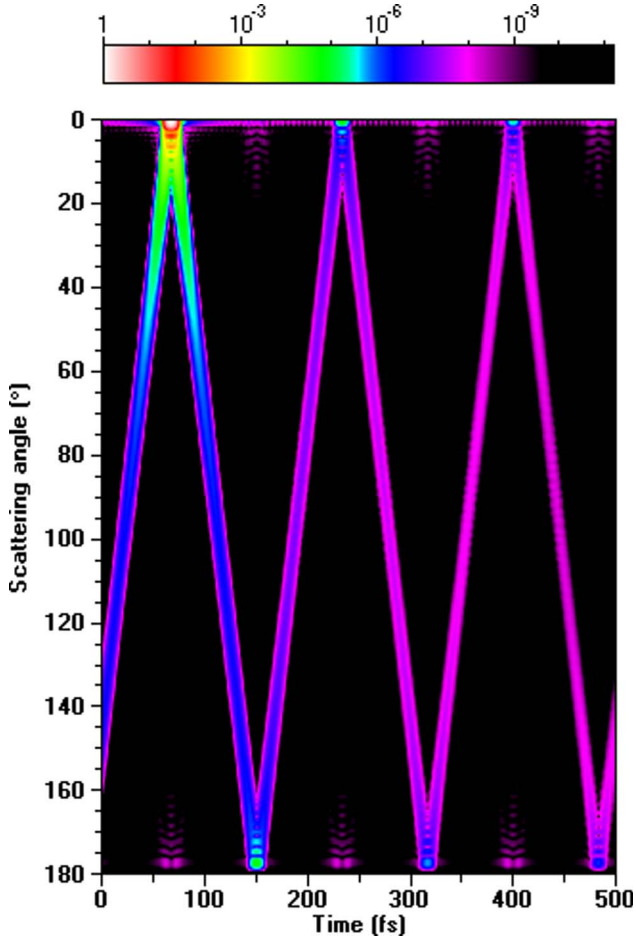

Fig. 5. (Color online) Diffracted intensity corresponding to Eq. (4) as a function of the scattering angle and delay time for the unpolarized raised cosine pulse of [29] with $\lambda_0 = 0.65\,\mu$m and $\tau = 10$ fs incident on a spherical particle of radius $a = 8\,\mu$m and refractive index $N + \mathrm{i}K = 1.3326 + \mathrm{i}(1.67 \times 10^{-8})$.

The sum formula can be modified to consider a finite sum of sampled values of the function $f(x)$, giving

$$\sum_{n=0}^{kA} f(x=n+1/2) = \sum_{m=-\infty}^{\infty} (-1)^m \int_0^{kA+1} \mathrm{d}x f(x) \exp(-2\pi i m x). \tag{43}$$

For the calculation of diffraction, the function $f(x)$ is chosen so as to match the contribution of the partial wave n when $x = n + 1/2$. The choice of the function that accomplishes this is not unique. But for θ outside the glory region, perhaps the simplest function that meets this criterion for scalar wave diffraction is

$$f(x) = xP_{x-1/2}[\cos(\theta)]. \tag{44}$$

The virtue of this choice is that the integrals in Eq. (43) can be evaluated approximately when θ is not near the forward or glory regions. Parenthetically, for scattering of a normally incident plane wave by a cylinder, the integrals can be evaluated exactly for all scattering angles. The resulting sum over m is found to be more rapidly convergent than the original sum over partial waves [17,18], and each term in the m sum has a simple physical interpretation. Substituting Eq. (44) and the asymptotic form of the first term of Eq. (25) into Eq. (43), recognizing the result as a Fresnel integral, retaining the leading term of its asymptotic form, and replacing A by the actual particle radius gives

$$S^{\mathrm{diff}}(\theta) \approx T_0(\theta) + B_0(\theta) + \sum_{m=1}^{\infty} (-1)^m [T_m^+(\theta) + B_m^+(\theta) + T_m^-(\theta) + B_m^-(\theta)], \tag{45}$$

where

$$T_0(\theta) = (D/\theta) \exp[\mathrm{i}(ka+1)\theta - 3\pi\mathrm{i}/4], \tag{46a}$$

$$B_0(\theta) = (D/\theta) \exp[-\mathrm{i}(ka+1)\theta + 3\pi\mathrm{i}/4], \tag{46b}$$

$$T_m^+(\theta) = [D/(2\pi m + \theta)] \exp[\mathrm{i}(ka+1)(2\pi m + \theta) - 3\pi\mathrm{i}/4], \tag{46c}$$

$$B_m^+(\theta) = [D/(2\pi m + \theta)] \exp[-\mathrm{i}(ka+1)(2\pi m + \theta) + 3\pi\mathrm{i}/4], \tag{46d}$$

$$T_m^-(\theta) = [D/(2\pi m - \theta)] \exp[-\mathrm{i}(ka+1)(2\pi m - \theta) + \mathrm{i}\pi/4], \tag{46e}$$

$$B_m^-(\theta) = [D/(2\pi m - \theta)] \exp[\mathrm{i}(ka+1)(2\pi m - \theta) - \mathrm{i}\pi/4], \tag{46f}$$

$$D = \{(ka+1)/[2\pi \sin(\theta)]\}^{1/2}. \tag{47}$$

The T_0 and B_0 terms were already obtained in Eq. (33) from approximating the partial wave sum by an integral over an effective impact parameter. They were also pictorially modeled in Fig. 2, and together they gave the classical Fraunhofer diffraction formula of Eq. (28) for small θ. In the context of the Poisson sum formula, T_0 and B_0 are now the first two terms of the exact result. The $m \geq 1$ terms can be interpreted in light of the geometrical theory of diffraction [38,39] as describing an orbiting behavior that extends in the time domain to progressively larger positive and negative time delays. In the spirit of the point of view that led to Fig. 2, the terms T_m^+ and T_m^- can be pictorially modeled as diffracted rays incident at the top edge of the sphere that then orbit it for at least m and $m-1$ cycles at the radius $r = a(1 + 1/ka)$ clockwise or counterclockwise, before heading off tangentially from the orbiting path toward the far zone. Clockwise orbiting produces larger positive delay times and counterclockwise orbiting produces progressively more negative time delays. Similarly, the terms B_m^+ and B_m^- can be pictorially modeled as diffracted rays incident at the bottom of the sphere that then orbit clockwise or counterclockwise for at least m and $m-1$ cycles before heading off to the far zone. In this case, clockwise orbiting produces progressively more negative time delays and counterclockwise orbiting produces longer positive time delays. Since the diffracted field slowly falls off as $1/(2\pi m \pm \theta)$, one might expect that the diffracted rays orbit the sphere many times while slowly damping out. This orbiting behavior is apparent in Fig. 5. It should also be noted that the use of the Poisson sum formula in [17,18] led to the analogous interpretation of electromagnetic surface waves as orbiting the sphere any number of times before exiting to the far zone.

5. REORGANIZATION OF PARTIAL WAVES IN THE TRANSITION REGION

The time domain behavior of Eqs. (45)–(47) as shown in Fig. 5 is problematic since the orbiting extends to long positive and negative delay times. Since the delay times in Figs. 1 and 3–5 are given with respect to that of specular reflection of the central ray, negative delay times correspond to the appearance of the diffracted pulse before the incident pulse arrives at the sphere, which, at first sight, seemingly violates the causality condition for scattering [16]. Although the time domain plot of diffraction alone in Fig. 5 possesses this behavior, the time domain plot of the entire $p = 0$ scattering amplitude in Fig. 1 does not. Evidently, some feature of reflection must cancel away both the seemingly causality violating portion of diffracted orbiting and the continued orbiting for long positive delay times. The cancellation mechanism was derived in [13]. Consider the calculation leading to the external reflection surface wave fields of Eqs. (17)–(20) for $\theta > (2/ka)^{1/3}$. In order to obtain convergence of the partial wave sum as $n \to \infty$, the expression $1/2(1 - R_n^{\mathrm{TE}})$ and $1/2(1 - R_n^{\mathrm{TM}})$ in the edge region along with the $\exp[\mathrm{i}(n+1/2)\theta - 3\pi\mathrm{i}/4]$ portion of the angular functions was integrated as a function of ε between $-\varepsilon_{\max}$ and $\varepsilon_{\max}$. This integral is not known analytically, nor is it easily approximated. But if the limits of integration could be extended to $+\infty$ and $-\infty$, the resulting integral could then be converted to a contour integral in the complex plane and evaluated using the method of residues. Extending the upper limit from $\varepsilon_{\max}$ to $+\infty$ poses no problem. But changing the lower limit from $-\varepsilon_{\max}$ to $-\infty$ necessitates the inclusion of all partial waves below the edge region. This is not problematic for the $(-1/2)R_n^{\mathrm{TE}}$ and $(-1/2)R_n^{\mathrm{TM}}$ factors with $\exp[\mathrm{i}(n + 1/2)\theta - 3\pi\mathrm{i}/4]$ since the integrand contains no stationary points. But it is problematic for the $(1/2)$ factors with $\exp[\mathrm{i}(n+1/2)\theta - 3\pi\mathrm{i}/4]$ since integration of these terms would otherwise be used to obtain half of the diffraction amplitude of Eq. (33). As a result, the price one pays for

extending the integration region downward so as to evaluate the integral analytically and obtain the contribution of surface waves is to not have the partial wave sum of (1/2) with $\exp[\mathrm{i}(n+1/2)\theta - 3\pi\mathrm{i}/4]$ available for $1 \le n \le kA$ to produce half of the diffraction amplitude.

There is also the matter of the edge region contribution to $(1/2)(1-R_n^{\mathrm{TE}})$ and $(1/2)(1-R_n^{\mathrm{TM}})$ along with the $\exp[-\mathrm{i}(n+1/2)\theta + 3\pi\mathrm{i}/4]$ portion of the angular functions. For $\theta < (2/ka)^{1/3}$, the full $p=0$ amplitude in the upper half of the edge region plus the reflected portion alone in the lower

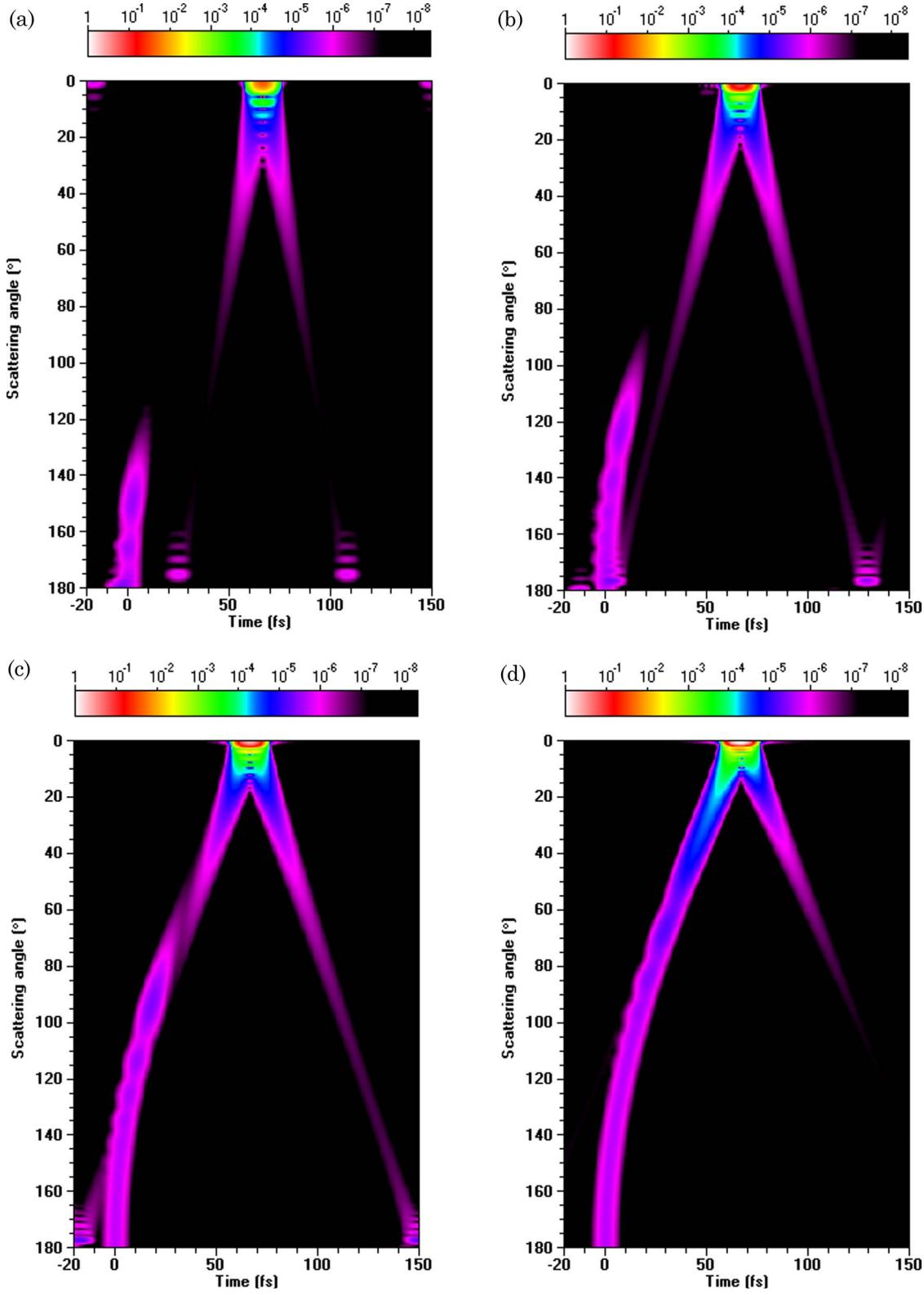

Fig. 6. (Color online) Intensity of the $p=0$ Mie–Debye term as a function of the scattering angle and delay time for the unpolarized raised cosine pulse of Fig. 5 incident on the spherical particle of Fig. 1. The upper limit of the Mie sum is (a) $0.4ka$, (b) $0.6ka$, (c) $0.8ka$, and (d) $1.0ka$.

half of the edge region was required in Eqs. (6a) and (6b) to obtain the near-forward grazing-plus-tunneling reflected field. But, for $\theta > (2/ka)^{1/3}$, the stationary point of the integrand of $(-1/2)R_n^{\mathrm{TE}}$ and $(-1/2)R_n^{\mathrm{TM}}$ that previously occurred at near-forward scattering angles for partial waves in the lower edge region has now migrated to larger scattering angles corresponding to partial waves far below the edge region. For these larger scattering angles, there is now no reason that the $(1/2)$ terms cannot be separated from the $(-1/2)R_n^{\mathrm{TE}}$ and $(-1/2)R_n^{\mathrm{TM}}$ terms in the upper half of the edge region. Appealing to Babinet's principle for plane wave incidence [41], the sum of the now-separated $(1/2)$ factor with $\exp[-(n+1/2)\theta + 3\pi\mathrm{i}/4]$ in the upper half of the edge region is equal and opposite to the $(1/2)$ factor with $\exp[-(n+1/2)\theta + 3\pi\mathrm{i}/4]$ summed for $1 \le n \le kA$, thus canceling away the other half of the diffraction amplitude of Eq. (33). When this argument is restated in the context of the Poisson sum formula [13], the entire orbiting structure of the diffraction amplitude is canceled away by the formation of external reflection surface waves for $\theta > (2/ka)^{1/3}$.

In the angular transition region $1/ka < \theta < (2/ka)^{1/3}$, the grazing-plus-tunneling reflection portion of the $p = 0$ amplitude may be written in terms of a number of Fock functions of the argument $\pm(ka/2)^{1/3}\theta$. For $\theta < 1/ka$, the argument of the Fock functions can be approximated by zero, giving the forward-focusing amplitude of Eq. (16). For $\theta > (2/ka)^{1/3}$, the Fock functions with positive argument are asymptotic to the surface wave amplitudes of Eqs. (17)–(20) and those with negative argument are asymptotic to the geometrical optics amplitudes of Eqs. (10a) and (10b). In the transition region, the diffraction amplitude is gradually replaced by what will eventually become the surface wave amplitude. This gradual evolution cannot be easily observed using the transitional approximations of Sections 3 and 4, but has been seen to occur smoothly in numerical computations using the more complicated uniform approximation to the $p = 0$ amplitude [35].

This evolution occurs very naturally in the time domain. Figures 6(a)–6(d) show the time domain intensity for $p = 0$, $\lambda_0 = 0.65\,\mu$m, and $a = 10\,\mu$m, but with the upper limit of the Mie sum being $0.4ka$, $0.6ka$, $0.8ka$, and $1.0ka$ rather than the computationally stable [42] upper limit $(ka) + \varepsilon_{\max}(ka)^{1/3}$ with $\varepsilon_{\max} = 4.05$. The decreased upper limits describe reflection of geometrical rays incident on an $a = 10\,\mu$m sphere with impact parameters out to 4, 6, 8, and $10\,\mu$m, accompanied by diffraction from a 4, 6, 8, and $10\,\mu$m radius sphere. As the upper limit of the Mie sum increases step by step, ray theory predicts that the specular reflection portion of the time domain intensity extends from 180° to 132.8°, then to 106.3°, 73.7°, and 0°. This agrees reasonably well with Figs. 6(a)–6(d). The figures also show that the inverted V structure of diffraction extends out to $\theta \approx 180°$, where it has glory interference structure consistent with J_2 dependence. As the effective sphere radius for diffraction increases, diffraction grows in strength so as to render the entire inverted V structure more clearly in the figures, and the opening angle of the inverted V increases as well. As the upper limit of the Mie sum approaches ka, the specular reflection intensity curves over toward the shorter-time arm of the inverted V of the diffracted intensity so that they meet up smoothly. At the same time, the longer-time arm of the inverted V arm weakens and shortens due to the reorganization of the partial waves described above. This gradually produces the dominance of external reflection surface waves seen in Fig. 1 for $\theta > (2/k_0a)^{1/3}$.

6. CONCLUSIONS

As was the case for the exactly soluble problem of scattering of a plane wave by an infinitesimally thin and perfectly conducting half-plane, one can give a precise definition of the physical process of diffraction in the context of the exactly soluble problem of Mie scattering. This definition is a consequence of a geometrical optics-based decomposition imposed on the total scattering amplitude. The diffracted amplitude thus defined is not a continuous function of particle size. The reflection part of the $p = 0$ Mie–Debye scattering amplitude was found to produce forward focusing, specular reflection, electromagnetic surface waves, and glory focusing in the appropriate angular regions, and its signature was examined in the time domain for scattering of a plane wave pulse. Diffraction was also studied in light of three different approaches to the exact amplitude. The uniform approximation to Legendre polynomials gave the classical Fraunhofer diffraction amplitude along with higher-order corrections that differ from those for scalar waves. The second approach used the Taylor series expansion of Legendre polynomials in the near-forward scattering region and led in the context of the geometrical theory of diffraction to the interpretation that diffracted rays travel slightly above the sphere surface. The third approach used the Poisson sum formula and led to the interpretation that diffraction is an orbiting phenomenon in the time domain that appears to violate the causality condition for scattering. The absence of this causality violating behavior in the entire $p = 0$ amplitude implies that, in the angular transition region $1/ka < \theta < (2/ka)^{1/3}$, diffraction is gradually cancelled by some feature of the reflected field.

Specifically, in the process of extending the integration limits over partial waves so as to obtain the contour integral describing external reflection surface waves, we used the partial waves that would have otherwise produced diffraction. Thus, the role in the $p = 0$ scattering amplitude that for $\theta < 1/ka$ was played by diffraction is now played for $\theta > (2/ka)^{1/3}$ by surface wave radiation. Figures 6(a)–6(d) illustrate the delicateness of this slow replacement in the time domain.

REFERENCES

1. D. Halliday, R. Resnick, and J. Walker, "Diffraction," in *Fundamentals of Physics*, 7th ed. (Wiley, 2005), p. 963.
2. E. Hecht, "Huygens principle," in *Optics*, 2nd ed. (Addison-Wesley, 1987), p. 80.
3. J. W. Goodman, "The Kirchhoff formula of diffraction by a plane screen," in *Introduction to Fourier Optics* (McGraw-Hill, 1968), pp. 37–42.
4. M. Born and E. Wolf, "Two-dimensional diffraction of a plane wave by a half-plane," in *Principles of Optics*, 6th ed. (Cambridge University, 1980), pp. 565–578.
5. M. Born and E. Wolf, "The nature of the solution," in *Principles of Optics*, 6th ed. (Cambridge University, 1980), p. 571.
6. M. Born and E. Wolf, "The nature of the solution," in *Principles of Optics*, 6th ed. (Cambridge University, 1980), p. 572.
7. M. Born and E. Wolf, "Expression of the solution in ters of Fresnel integrals," in *Principles of Optics*, 6th ed. (Cambridge University, 1980), p. 569.
8. H. C. van de Hulst, "Rigorous scattering theory for spheres of arbitrary size," in *Light Scattering by Small Particles* (Dover, 1957), pp. 114–130.

9. M. Kerker, "Scattering by a sphere," in *The Scattering of Light and Other Electromagnetic Radiation* (Academic, 1969), pp. 27–96.
10. C. F. Bohren and D. R. Huffman, "Absorption and scattering by a sphere," in *Absorption and Scattering of Light by Small Particles* (Wiley, 1983), pp. 82–129.
11. B. Van der Pol and H. Bremmer, "The diffraction of electromagnetic waves from an electrical point source round a finitely conducting sphere, with applications to radiotelegraphy and the theory of the rainbow," Philos. Mag. **24**, 825–864 (1937).
12. H. C. van de Hulst, "The diffraction part," in *Light Scattering by Small Particles* (Dover, 1957), p. 209.
13. H. M. Nussenzveig, "Uniform approximation in scattering by spheres," J. Phys. A **21**, 81–109 (1988), Section 4.2.
14. J. A. Lock and E. A. Hovenac, "Diffraction of a Gaussian beam by a spherical obstacle," Am. J. Phys. **61**, 698–707 (1993).
15. H. M. Nussenzveig, "The Debye expansion," in *Diffraction Effects in Semiclassical Scattering* (Cambridge University, 1992), p. 96.
16. E. P. Wigner, "Lower limit for the energy derivative of the scattered phase shift," Phys. Rev. **98**, 145–147 (1955).
17. H. M. Nussenzveig, "High-frequency scattering by an impenetrable sphere," Ann. Phys. **34**, 23–95 (1965).
18. H. M. Nussenzveig, "High-frequency scattering by a transparent sphere. I. Direct reflection and transmission," J. Math. Phys. **10**, 82–124 (1969).
19. V. Khare, "Short-wavelength scattering of electromagnetic waves by a homogeneous dielectric sphere," Ph.D. dissertation (University of Rochester, 1976), pp. 89–109.
20. M. Abramowitz and I. A. Stegun, eds., *Handbook of Mathematical Functions* (National Bureau of Standards, 1964), p. 366 Eq. (9.3.4), p. 448 Eq. (10.4.59), p. 449 Eq. (10.4.63).
21. M. Abramowitz and I. A. Stegun, eds., *Handbook of Mathematical Functions* (National Bureau of Standards, 1964), p. 366 Eq. (9.3.4), p. 448 Eq. (10.4.60), p. 449 Eq. (10.4.64).
22. M. Abramowitz and I. A. Stegun, eds., *Handbook of Mathematical Functions* (National Bureau of Standards, 1964), p. 366 Eq. (9.3.3).
23. H. C. van de Hulst, "The reflected and refracted light," in *Light Scattering by Small Particles* (Dover, 1957), p. 212.
24. K. W. Ford and J. A. Wheeler, "Semiclassical description of scattering," Ann. Phys. **7**, 259–286 (1959).
25. D. Q. Chowdhury, S. C. Hill, and P. W. Barber, "Time dependence of internal intensity of a dielectric sphere on or near resonance," J. Opt. Soc. Am. A **9**, 1364–1373 (1992).
26. E. E. M. Khaled, D. Q. Chowdhury, S. C. Hill, and P. W. Barber, "Internal and scattered time-dependent intensity of a dielectric sphere illuminated with a pulsed Gaussian beam," J. Opt. Soc. Am. A **11**, 2065–2071 (1994).
27. K. S. Shifrin and I. G. Zolotov, "Quasi-stationary scattering of electromagnetic pulses by spherical particles," Appl. Opt. **33**, 7798–7804 (1994).
28. P. Laven, "Separating diffraction from scattering: the million-dollar challenge," J. Nanophoton. **4**, 041593 (2010).
29. J. A. Lock and P. Laven, "Mie scattering in the time domain. Part I. The role of surface waves," J. Opt. Soc. Am. A **28**, 1086–1095 (2011).
30. J. A. Lock, "Observability of atmospheric glories and supernumerary rainbows," J. Opt. Soc. Am. A **6**, 1924–1930 (1989).
31. M. Abramowitz and I. A. Stegun, eds., "Bessel functions of fractional order," in *Handbook of Mathematical Functions* (National Bureau of Standards, 1964), p. 478, Table 10.13.
32. H. C. van de Hulst, "Theory based on Mie's formulae," in *Light Scattering by Small Particles* (Dover, 1957), p. 253.
33. G. Arfken, "Recurrence relations and special properties," in *Mathematical Methods for Physicists*, 3rd. ed. (Academic, 1985), p. 648 Eq. (12.28).
34. J. J. Bowman, T. B. A. Senior, and P. L. E. Uslenghi, "Legendre functions," in *Electromagnetic and Acoustic Scattering by Simple Shapes* (Hemisphere, 1969), p. 76 Eqs. (1.367, 1.369).
35. H. M. Nussenzveig and W. J. Wiscombe, "Complex angular momentum approximation to hard-core scattering," Phys. Rev. A **43**, 2093–2112 (1991).
36. J. J. Bowman, T. B. A. Senior, and P. L. E. Uslenghi, "Legendre functions," in *Electromagnetic and Acoustic Scattering by Simple Shapes* (Hemisphere, 1969), p. 72 Eq. (1.335).
37. G. Arfken, "Asymptotic expansions," in *Mathematical Methods for Physicists*, 3rd ed. (Academic, 1985), p. 620 Eq. (11.137).
38. J. B. Keller, "A geometrical theory of diffraction," in *Calculus of Variations and Its Applications*, Proceedings of Symposia in Applied Mathematics, L. M. Graves, ed. McGraw-Hill, 1958), Vol. 3, pp. 27–52.
39. J. B. Keller, "Diffraction by an aperture," J. Appl. Phys. **28**, 426–444 (1957).
40. P. M. Morse and H. Feshbach, "Poisson sum formula," in *Methods of Theoretical Physics* (McGraw-Hill, 1953), pp. 466–467.
41. E. Hecht, "Babinet's principle," in *Optics*, 2nd ed. (Addison-Wesley, 1987), pp. 458–459.
42. W. J. Wiscombe, "Improved Mie scattering algorithms," Appl. Opt. **19**, 1505–1509 (1980).